CHAPTER 6

DESIGN OF TCM AND MTCM FOR FADING CHANNELS

In this chapter the design of Multiple-Trellis Coded Modulation (MTCM) for Q^2PSK is presented when transmitted over a fading channel. Although, both Rician and Rayleigh fading channels are considered, most of this section is concerned with the design for transmission over the Rician channel. The latter choice has been made in view of the fact that the distortion introduced by the Rayleigh channel requires the use of an adaptive equaliser which does not form part of this study.

Digital communications over mobile channels often suffers from multipath effects, which results in signal fading. Multipath fading plagues the propagation medium by imposing random amplitude and phase variations onto the transmitted waveform. It is well known that this fading degrades the performance of the communications systems. Therefore, this research is primarily concerned with the application of MTCM to Q^2PSK in order to achieve superior performance on the fading channel, compared to that achievable by conventional (single channel symbol per trellis branch) TCM of the same throughput and decoder complexity.

Divsalar and Simon did some excellent work on the effects of fading in M-PSK signals [39, 81]. They showed that whereas maximising free Euclidean distance (d_{free}) is the optimum criterion on the AWGN channel, in the case of fading channels (specifically Rician) with interleaving/deinterleaving, the asymptotic (high SNR) performance of TCM is dominated by several other factors. These factors are catagorised as primary and secondary considerations and depends on the value of the Rician parameter, K. Specifically, for small values of K, the primary design criteria become

- the *length* of the shortest error event path (measured in number of symbols), and

- the *product* of branch distances along that path, with d_{free} a secondary consideration.

As K increases, the significance of these primary and secondary considerations shift relative to one another until K reaches infinity (AWGN channel), in which case optimum performance is once again achieved by trellis code designed solely to maximise d_{free}.

In this section attention is focused on implementing the foregoing considerations in the design and implementation of trellis codes for Q^2PSK to give optimum performance on the fading channel. The design of Multiple Trellis Coded Modulation (MTCM) codes is considered, since the diversity potential offered by the latter codes is fully exploited by the fading channel.

6.1 MULTIPLE TRELLIS CODED MODULATION

Recall that with conventional trellis coding (i.e., one symbol per trellis branch), the length L of the shortest EEP is equal to the number of trellis branches along that path. Equivalently, if it is assumed that the all-zeros path in the trellis diagram represents the transmitted sequence, L is the number of branches in the shortest path to which a nonzero symbol is associated. Since a trellis diagram with parallel paths is constrained to have a shortest error event path of one branch, thus $L = 1$. This implies that asymptotic region of the graph of expected (average) bit error probability will vary *inverse linearly* with $\overline{E_s}/N_o$ or E_s/N_o, since $\overline{E_s} = E_s$ [30]. Therefore, from an error probability viewpoint it is undesirable to design conventional TCM codes to have parallel paths in their trellis diagrams. Unfortunately, for a convolutional code of rate $m/(m+1)$, when 2^m exceeds the number of states, one is forced to utilise a trellis containing parallel paths.

When MTCM is employed, the option of designing a trellis diagram with parallel paths may again be considered, since achieving an asymptotic performance on the fading channel which varies inversely with $\overline{E_s}/N_o$ at a rate faster than linear may now be achieved. The reason behind this lies in the fact that even if parallel paths exist in the trellis, it is now possible to have more than one coded symbol with nonzero Euclidean distance associated with an EEP branch of length, $L = 1$.

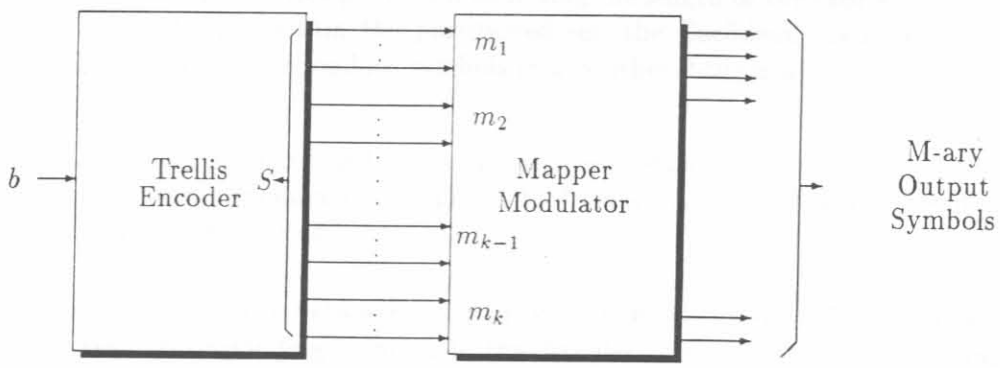

Figure 6.1: Generalised MTCM transmitter.

In its most general form, MTCM is implemented by an encoder with b binary input bits and s binary output bits that are mapped into k Q^2-ary symbols in each transmission interval, illustrated in Figure 6.1. The parameter k is referred to as the *multiplicity* of the code, since it represents the number of Q^2-ary symbols allocated to each branch in the trellis diagram ($k = 1$ corresponds to conventional TCM). To produce such a result, the s binary encoder output bits are partitioned into k groups containing $m_1, m_2, \ldots, m_k$ symbols. Each of these groups, through a suitable mapping function, results in an Q^2-ary output symbol. The transmitter parameters are constrained such that

$$s = k \log_2 M \tag{6.1}$$

where $M = 16$ for Q^{2}PSK, without expanded signal set (note that $M = 32$ when an expanded signal set is utilised). The throughput of the MTCM transmitter is given by $r = b/k$ *bits/s/Hz*, which is not necessarily integer-valued.

6.1.1 Ungerboeck Set Partitioning: From *Root-to-Leaf*

In the design of the trellis codes a procedure similar to that presented in [30], known as the *Ungerboeck: Root-to-Leaf* approach, has been followed. The method, makes use of k-fold Cartesian products of the sets found in Ungerboeck's original set-partitioning method for conventional trellis codes [27]. The set-partitioning procedure is started with a k-fold Cartesian product of the complete Q^{2}PSK signal set.

Attention is focused on the design of a code with multiplicity, $k = 2$. Let A_0 denotes the complete Q^{2}PSK signal set (i.e., signal points $0, 1, \ldots, M-1 = 15$) and $A_0 \otimes A_0$ denote the two-fold Cartesian product of A_0 with itself. (Note, that for a multiplicity, $k = 4$, the process should have started with the four-fold Cartesian product set, $A_0 \otimes A_0 \otimes A_0 \otimes A_0$). Thus, an element of the set $A_0 \otimes A_0$ is a 2-tuple, denoted by (j_1, j_2), with symbols chosen from the set A_0. The first step is to partition $A_0 \otimes A_0$ into M signal sets defined by the ordered Cartesian product $\{A_0 \otimes B_i\}$, $i = 0, 1, \ldots, M-1$. The second element $\{j_2\}$ of B_i is defined by $nj + i \mod M$. Thus, the j-th 2-tuple from the product $A_0 \otimes B_i$ is the ordered pair $(j_1 = j, j_2 = nj + i)$.

The first partitioning step has two purposes. These are summarised below [30]:

- Firstly, it guarantees that within any of the M partitions, each of the two symbol positions has distinct elements, from the viewpoint of maximising the length of the shortest error event path. That is, for a 2-tuple within the partitioned set, the Euclidean distance of each of the two symbols from the corresponding symbols in any other 2-tuple within the same set is nonzero.

- Secondly, it accomplishes a minimum Euclidean distance *product* between 2-tuples within the partitioned set (i.e., the minimum of the product of the distances between corresponding 2-tuple symbol pairs) is maximised.

Since the squared Euclidean distance between any pair of 2-tuples is the sum of the squared Euclidean distances between corresponding symbols in the 2-tuples, the set partitioning guarantees that the *intradistance* (i.e., distance between pairs within a specific set or partition) of all of the partitions $A_0 \otimes B_i$ is identical. It is, therefore, sufficient to study the distance structure of $A_0 \otimes B_0$, referred to as the *generating set* by Biglieri et al.[30]. For this set, the minimum product of squared distances over all pairs of 2-tuples in $A_0 \otimes B_0$, $\prod d_{ij}^2$ must be maximised. This is done by choosing the odd integer multiplier, n such that it produces a *maximin* solution. A computer search for possible values of n to be utilised, revealed the solution as $n = 11$. In [30] it was stated that the *additive inverse* of n, denoted by $n^* = M - n$, could also have been used. However, in our design the solution for n^* does not produce optimum (i.e., maximum) intradistances. The ordered Cartesian product set, $A_0 \otimes A_0$, together with the generating set, $A_0 \otimes B_0$ are illustrated below for Q^2PSK with $M = 16$.

$$A_0 \otimes A_0 = \begin{bmatrix} 0 & 0 & 8 & 8 \\ 1 & 1 & 9 & 9 \\ 2 & 2 & 10 & 10 \\ 3 & 3 & 11 & 11 \\ 4 & 4 & 12 & 12 \\ 5 & 5 & 13 & 13 \\ 6 & 6 & 14 & 14 \\ 7 & 7 & 15 & 15 \end{bmatrix} \qquad A_0 \otimes B_0 = \begin{bmatrix} 0 & 0 & 8 & 8 \\ 1 & 11 & 9 & 3 \\ 2 & 6 & 10 & 14 \\ 3 & 1 & 11 & 9 \\ 4 & 12 & 12 & 4 \\ 5 & 7 & 13 & 15 \\ 6 & 2 & 14 & 10 \\ 7 & 13 & 15 & 5 \end{bmatrix} \tag{6.2}$$

The sets obtained by this first partition, each with minimum intradistance of $8.0E_b$, are illustrated in Appendix D, for $n = 11$. The *interdistances* (i.e., minimum distances between pairs of 2-tuples from different sets), for these sets are summarised in Table 6.1 below.

Table 6.1: Interdistances between partitioned subsets, with $A_0 \otimes B_0$ used as reference.

Subset	Distance	Subset	Distance
$A_0 \otimes B_0$	—	$A_0 \otimes B_8$	$4.0E_b$
$A_0 \otimes B_1$	$4.0E_b$	$A_0 \otimes B_9$	$8.0E_b$
$A_0 \otimes B_2$	$4.0E_b$	$A_0 \otimes B_{10}$	$8.0E_b$
$A_0 \otimes B_3$	$8.0E_b$	$A_0 \otimes B_{11}$	$8.0E_b$
$A_0 \otimes B_4$	$4.0E_b$	$A_0 \otimes B_{12}$	$4.0E_b$
$A_0 \otimes B_5$	$8.0E_b$	$A_0 \otimes B_{13}$	$8.0E_b$
$A_0 \otimes B_6$	$8.0E_b$	$A_0 \otimes B_{14}$	$4.0E_b$
$A_0 \otimes B_7$	$8.0E_b$	$A_0 \otimes B_{15}$	$4.0E_b$

The second step in the set partitioning procedure for MTCM design also differs somewhat from the traditional set partitioning procedure. The second step should guarantee that the resulting sets, of dimensionality $M/2$, have an intradistance product structure equal to that achieved by the first-level partitioning in occordance with the requirement to achieve a *maximin* Euclidean distance. In the second step of set partitioning M is replaced by $M/2$.

In order to perform the set partitioning, another odd integer multiplier, denoted by n' is introduced such that it again results in a maximin solution. A computer search revealed the optimum solution for the second level multiplier as $n' = 3$. Note that if one of the solutions for n' (or its additive inverse n'^{*} [1]) is equal to the solution of the first level multiple, n, when M is replaced by $M/2$, then the first two levels follow a *tree structure*. Since, this is not the case here, the sets formed by the second level partition have to be recalculated, repeating the procedure followed in the first partitioning. The two subsets, $C_0 \otimes D_{0a}$ and $C_0 \otimes D_{0b}$, resulting from partitioning set $A_0 \otimes B_0$, are shown in (6.3); the complete partitioned subsets are given in Appendix D. The *interdistances* for these sets, with reference to subset $C_0 \otimes D_{0a}$, are summarised in Table 6.2 below. Each of the subsets have a minimum intradistance of $8.0E_b$, corresponding to the sets formed by the first partitioning step.

[1] Additive inverse, n'^{*} is given as $M - n'$.

$$C_0 \otimes D_{0a} = \begin{bmatrix} 0 & 0 & 4 & 8 \\ 1 & 6 & 5 & 14 \\ 2 & 12 & 6 & 4 \\ 3 & 2 & 7 & 10 \end{bmatrix} \quad C_0 \otimes D_{0b} = \begin{bmatrix} 0 & 3 & 4 & 11 \\ 1 & 9 & 5 & 1 \\ 2 & 15 & 6 & 7 \\ 3 & 5 & 7 & 13 \end{bmatrix} \tag{6.3}$$

Table 6.2: Interdistances between partitioned subsets, with $C_0 \otimes D_{0a}$ used as reference.

Subset	Distance	Subset	Distance
$C_0 \otimes D_{0a}$	—	$C_0 \otimes D_{0b}$	$12.0E_b$
$C_0 \otimes D_{1a}$	$4.0E_b$	$C_0 \otimes D_{1b}$	$12.0E_b$
$C_0 \otimes D_{2a}$	$4.0E_b$	$C_0 \otimes D_{2b}$	$16.0E_b$
$C_0 \otimes D_{3a}$	$8.0E_b$	$C_0 \otimes D_{3b}$	$12.0E_b$
$C_0 \otimes D_{4a}$	$4.0E_b$	$C_0 \otimes D_{4b}$	$16.0E_b$
$C_0 \otimes D_{5a}$	$8.0E_b$	$C_0 \otimes D_{5b}$	$12.0E_b$
$C_0 \otimes D_{6a}$	$4.0E_b$	$C_0 \otimes D_{6b}$	$12.0E_b$
$C_0 \otimes D_{7a}$	$4.0E_b$	$C_0 \otimes D_{7b}$	$8.0E_b$
$C_0 \otimes D_{8a}$	$0.0E_b$	$C_0 \otimes D_{8b}$	$12.0E_b$
$C_0 \otimes D_{9a}$	$4.0E_b$	$C_0 \otimes D_{9b}$	$12.0E_b$
$C_0 \otimes D_{10a}$	$4.0E_b$	$C_0 \otimes D_{10b}$	$16.0E_b$
$C_0 \otimes D_{11a}$	$8.0E_b$	$C_0 \otimes D_{11b}$	$12.0E_b$
$C_0 \otimes D_{12a}$	$4.0E_b$	$C_0 \otimes D_{12b}$	$16.0E_b$
$C_0 \otimes D_{13a}$	$8.0E_b$	$C_0 \otimes D_{13b}$	$12.0E_b$
$C_0 \otimes D_{14a}$	$4.0E_b$	$C_0 \otimes D_{14b}$	$12.0E_b$
$C_0 \otimes D_{15a}$	$4.0E_b$	$C_0 \otimes D_{15b}$	$8.0E_b$

The set partitioning procedure is illustrated in Figure 6.2 for $k = 2$. To extend the previous procedure to higher multiplicity of order $k \geq 2$, simply form the $k/2$-fold ordered Cartesian product of all the sets on a given partition level created by the procedure for $k = 2$. The result of this procedure is illustrated in Figure 6.3 for $k = 4$.

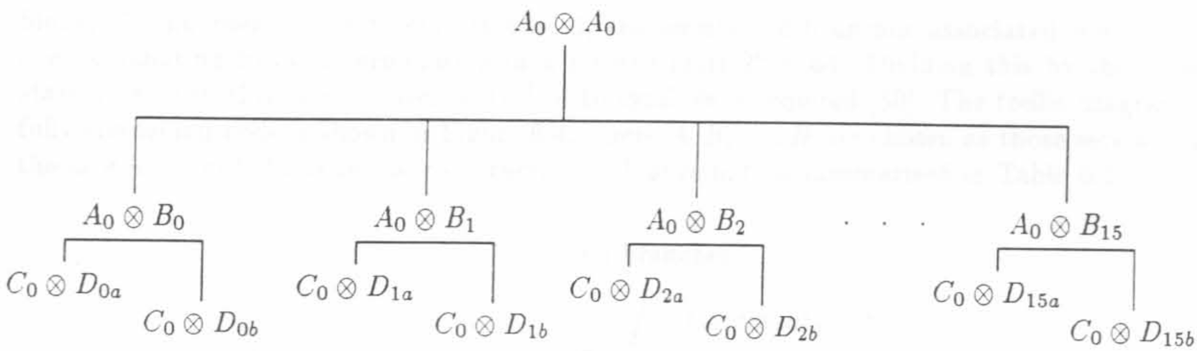

Figure 6.2: Set partitioning method for multiple ($k = 2$) trellis codes on the fading channel.

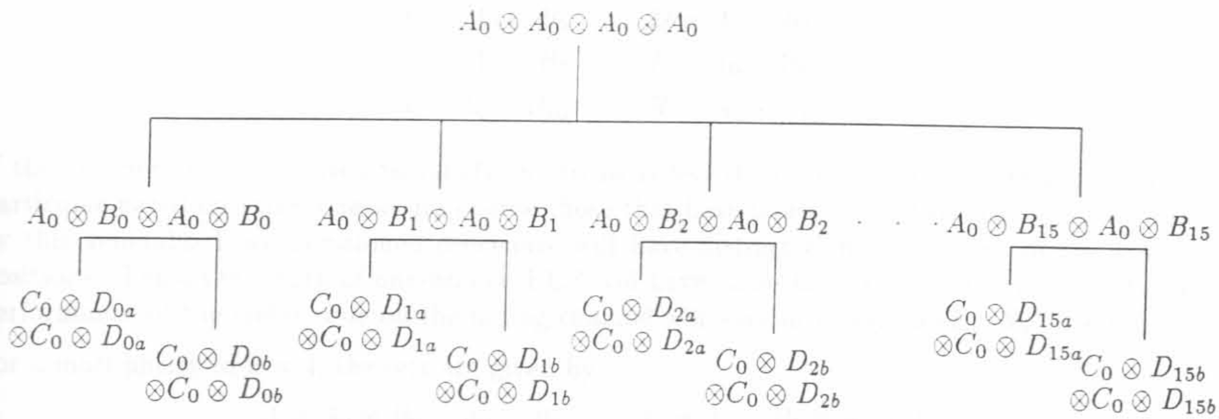

Figure 6.3: Set partitioning method for multiple ($k = 4$) trellis codes on the fading channel.

6.2 Q^2PSK/MTCM CODE DESIGN

6.2.1 Design of 4-State Rate 6/8 codes

In this section the design of a 4-state trellis code, with multiplicity $k = 2, 4$, is discussed. Two Q^2PSK symbols are transmitted over the channel for each 6 bits accepted by the encoder. Hence, the throughput of the system is lowered by a factor 8/6, resulting in a spectral efficiency of 1.5 *bits/s/Hz*, compared to the 2.0 *bits/s/Hz* of the uncoded system.

Since, the number of input bits are $b = 6$, the number of branches associated with each state (i.e., emanating from or terminating in a node) equals $2^6 = 64$. Dividing this by the number of states, i.e., 4 in this case, a cardinality [2] of 16 symbols is required [30]. The trellis diagram of this fully-connected code is shown in Figure 6.4, where $A, B, \ldots, H$ are chosen as those sets which have the largest *interdistance* in the construction of Figure 6.2, as summarised in Table 6.1.

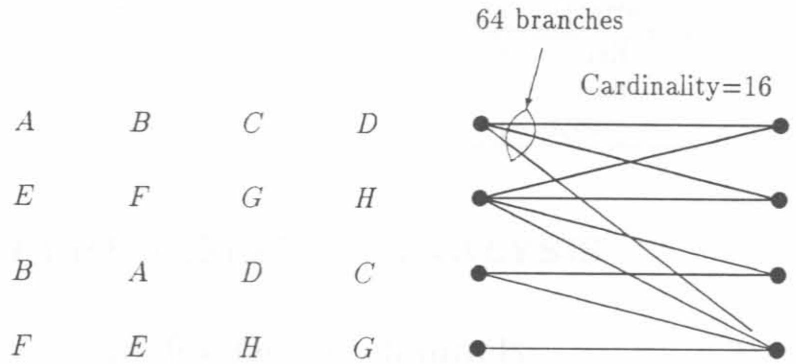

Figure 6.4: Rate-6/8 4-state Q^2PSK/MTCM

Thus, for a multiplicity of $k = 2$, the sets are given by

$$\begin{aligned} A &= A_0 \otimes B_0 \quad , \quad B = A_0 \otimes B_3 \\ C &= A_0 \otimes B_5 \quad , \quad D = A_0 \otimes B_6 \\ E &= A_0 \otimes B_7 \quad , \quad F = A_0 \otimes B_9 \\ G &= A_0 \otimes B_{10} \quad , \quad H = A_0 \otimes B_{11} \end{aligned} \tag{6.4}$$

If the number of sets required to satisfy the trellis is less than the number of sets generated on a particular partition leave, one would choose those that have largest *interdistance*. The sets formed by this generalised set-partitioned procedure will have distinct elements in any of the k symbol positions. Thus, the length of one-branch EEP will have value k, and hence the asymptotic BER performance of the trellis code on the fading channel will vary inversely as $(\overline{E_s}/N_o)^n$, with $n \geq k$.

For a multiplicity of $k = 4$, the sets are given by

$$\begin{aligned} A &= A_0 \otimes B_0 \otimes A_0 \otimes B_0 \quad , \quad B = A_0 \otimes B_3 \otimes A_0 \otimes B_3 \\ C &= A_0 \otimes B_5 \otimes A_0 \otimes B_5 \quad , \quad D = A_0 \otimes B_5 \otimes A_0 \otimes B_6 \\ E &= A_0 \otimes B_7 \otimes A_0 \otimes B_7 \quad , \quad F = A_0 \otimes B_9 \otimes A_0 \otimes B_9 \\ G &= A_0 \otimes B_{10} \otimes A_0 \otimes B_{10} \quad , \quad H = A_0 \otimes B_{11} \otimes A_0 \otimes B_{11} \end{aligned} \tag{6.5}$$

[2] The cardinality is a number used to represent the size of a subset.

Several MTCM code designs were carried out. The designs are summarised in Table 6.3.

Table 6.3: Design summary for Q^2PSK/MTCM.

Code Rate R_c	Branches per State	Number of States	Connectivity	Multiplicity k	Required Cardinality
6/8	64	4	Fully	2	≥ 16
5/8	32	4	Fully	2	≥ 8
4/8	16	4	Half	2	≥ 8
6/16	64	4	Fully	4	≥ 16
5/16	32	4	Fully	4	≥ 8
4/16	16	4	Half	4	≥ 8
6/8	64	8	Half	2	≥ 8
5/8	32	8	Half	2	≥ 4
4/8	16	8	Quarter	2	≥ 4
6/16	64	8	Half	4	≥ 8
5/16	32	8	Half	4	≥ 4
4/16	16	8	Quarter	4	≥ 4

6.3 PERFORMANCE ANALYSIS

6.3.1 TCM for fading channels

It was shown by Biglieri et al. [30] that the asymptotic pairwise error performance for coherent detection varies inversely with $(E_s/N_0)^{L_\eta}$. L_η is the smallest number of elements with non-zero pairwise distances between the symbols along its branches and those along the correct path. Evaluation of the pairwise probability depends on the proposed decoding metric, the presence or absence of Channel State Information (CSI), and the type of detection used. In [30] the relation between the asymptotic behavior of the pairwise error probability to that of the BEP is approximately given by

$$P_b \cong \frac{1}{b} C \left(\frac{(1+K)e^{-K}}{E_s/N_0} \right)^{L_\eta}, \quad E_s/N_o \gg K \tag{6.6}$$

where b is the number of bits transmitted per branch in the trellis, K is the Rician parameter and C is a constant that depends on the distance structure of the code, defined as [30]

$$C = \begin{cases} 4^{L_\eta} \left[\prod_{n\epsilon\eta} \mid x_n = \hat{x_n} \mid^2 \right]^{-1} & \text{Coherent detection with ideal CSI} \\ \left(\frac{2e}{L_\eta}\right)^{L_\eta} \left(\prod_{n\epsilon\eta} \frac{|x_n = \hat{x}_n|^2}{\left(\sum_{n\epsilon\eta} |x_n = \hat{x}_n|^2\right)^{1/2}} \right)^{-2} & \text{Coherent detection with no CSI} \end{cases} \tag{6.7}$$

From the above it may be concluded that the primary objective for good trellis code design on the fading channel is the maximisation of the number of symbols with non-zero ED between the error and correct paths, denoted by L_η.

As an example the rate-3/4 trellis coded Q^2PSK with 8-state trellis diagram is considered, corresponding to the design carried out in the previous chapter (see Figure 5.14). Referring to the state diagram of Figure 5.14, the shortest EEP branches is of length, $L = 3$, and all of these have nonzero distance with respect to the branches of the correct path (assumed to be the all-zeros path). Thus the length L of the shortest EEP equals 3, or equivalently, the code has a diversity equal to 3.

For coherent detection with no CSI, the product of the squared branch distances need to be computed, normalised by the square root of their sum in accordance with C of (6.7). From Figure 5.14, the square of this ratio is easily computed as

$$\left(\prod_{n \epsilon \eta} \frac{|x_n - \hat{x}_n|^2}{\left(\sum_{n \epsilon \eta} |x_n - \hat{x}_n|^2\right)^{1/2}}\right)^{-2} = \left[\frac{4 \cdot 8 \cdot 4}{(4+8+4)^{3/2}}\right]^{-2} = \frac{1}{4} \qquad (6.8)$$

Thus letting $L_\eta = 3$ and $b = 3$ in (6.6), the approximated average BEP in terms of E_b/N_o and K is

$$P_b \cong \frac{2e^3}{81}\left(\frac{(1+K)e^{-K}}{E_b/N_o}\right)^3 \qquad (6.9)$$

for $E_b/N_o \gg K$.

For coherent detection with CSI, the product of the distances in accordance with C in (6.7) need to be computed. For the shortest EEP this product is easily computed as

$$\prod_{n \epsilon \eta} |x_n - \hat{x}_n|^2 = 4 \cdot 8 \cdot 4 = 128 \qquad (6.10)$$

Substituting this value for C into (6.6), the BEP is given by

$$P_b \cong \frac{1}{6}\left(\frac{(1+K)e^{-K}}{E_b/N_o}\right)^3 \qquad (6.11)$$

6.3.2 MTCM for fading channels

The throughput of multiple trellis codes can be compared with the computational cutoff rate R_o of the decoding channel to determine the efficiency of the code design. The computation of R_o, which is very similar to the channel capacity C discussed in Chapter 2, in not at all straight forward. In fact, it is an extremely complex process. For this reason the theoretical analysis has been omitted. The efficiency of the MTCM designs will therefore only be evaluated by means of computer simulation. In the following chapter these MTCM coding designs will be subjected to extensive simulations.

6.4 CONCLUDING REMARKS: CHAPTER 6

Optimum design criteria for trellis coded Q^2PSK systems on fading channels have been derived and presented in this chapter. These criteria were utilised in the designs of new multiple trellis coded Q^2PSK systems.

Initially, the study model of the coded Q^2PSK system on the fading channel has been presented. Fading channel statistics have been analysed and utilised in the design of the trellis coded systems. Design criteria derivation has revealed that design of trellis coded Q^2PSK systems to achieve optimum performance on the Rician fading channel is guided by factors that differ from optimum code design on the AWGN channel. In particular, to minimise the error probability, the code has to maximise the length of symbols at nonzero Euclidean distance from the shortest EEP. The secondary objective is to maximise the product of the branch distances along the shortest EEP, normalised by the Euclidean distance if coherent detection is utilised. The final objective will be the maximisation of the free squared Euclidean distance of the code. However, the relative importance of these parameters varies with the variation of the Rician factor encountered on the Rician fading channel.

Several new TCM and MTCM trellis codes for Q^2PSK signals have been designed and constructed. In the next chapter these coding schemes will be subjected to extensive simulation tests on the AWGN channel, as well as to fading channel conditions, to establish comparitive coding efficiencies.